Exploiting Non-Radiating Currents to Design Reflectarrays with Arbitrary Geometrical Constraints

M. Salucci, A. Gelmini, G. Oliveri, N. Anselmi, and A. Massa

Abstract

This work presents an innovative methodology for synthesizing the reflectarray surface current that is able to meet (at the same time) radiation and user-defined geometrical constraints. Towards this end, by suitably formulating the reflectarray design as an inverse source (*IS*) problem, the *non-radiating* current components flowing on the reflective surface are profitably determined in order to cancel the overall current in correspondence to selected sub-regions (i.e., "*forbidden-regions*") of the antenna surface without modifying the desired radiation features. Representative numerical results are shown to validate the effectiveness of the developed synthesis method.

Contents

1 Numerical Results

1.1 Shape "O @ Center"

Parameters

- Number of reflectarray elements: $M = N = 55$;
- Operative frequency: $f = 14$ [GHz];
- Polarization: X-CO;
- Number of elements in the forbidden region: $Q = 24$;

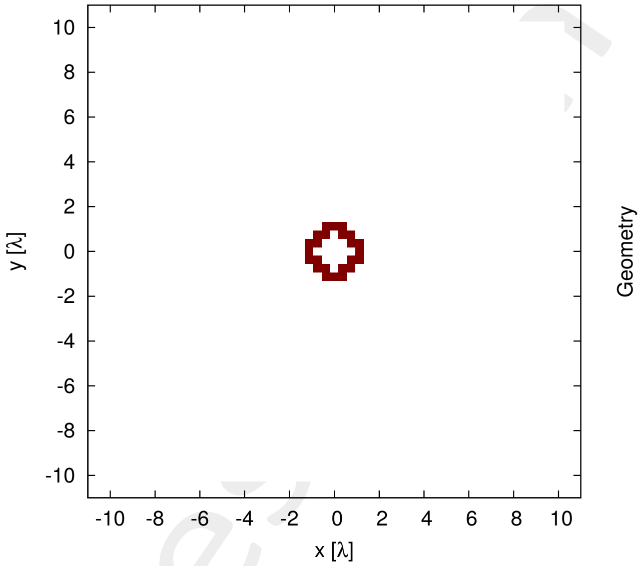

Figure 1: Geometry of forbidden region Ω.

Results

Magnitude and phase of the *NR* coefficients.

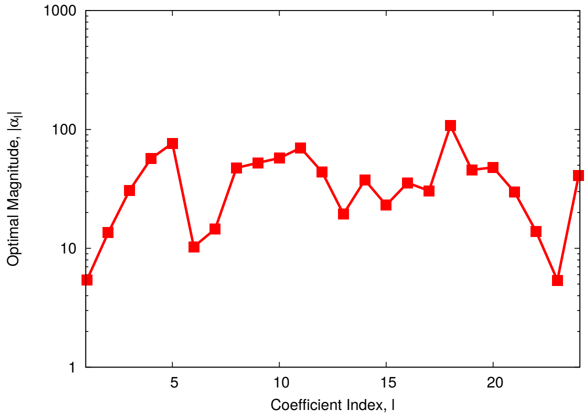

(a)

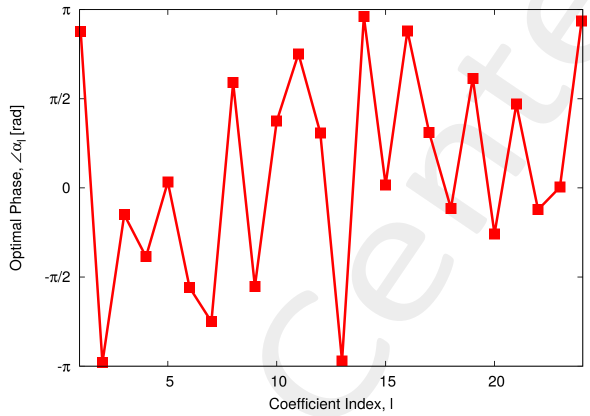

(b)

Figure 2: Magnitude (a) and phase (b) of the solution.

Index q	$\Re\{\alpha_q\}$	$\Im\{\alpha_q\}$	Index q	$\Re\{\alpha_q\}$	$\Im\{\alpha_q\}$
1	-4.99	2.03	13	-1.93×10^1	-1.77
2	-1.35×10^1	-8.46×10^{-1}	14	-3.73×10^1	4.67
3	2.74×10^1	-1.40×10^1	15	2.30×10^1	1.28
4	1.99×10^1	-5.32×10^1	16	-3.31×10^1	1.30×10^1
5	7.61×10^1	7.93	17	1.71×10^1	2.52×10^1
6	-1.90	-1.01×10^1	18	1.01×10^2	-3.80×10^1
7	-1.03×10^1	-1.03×10^1	19	-1.61×10^1	4.27×10^1
8	-1.32×10^1	4.56×10^1	20	3.31×10^1	-3.48×10^1
9	-8.58	-5.17×10^1	21	2.85	2.96×10^1
10	2.21×10^1	5.30×10^1	22	1.29×10^1	-5.23
11	-4.99×10^1	4.91×10^1	23	5.39	6.66×10^{-2}
12	2.48×10^1	3.62×10^1	24	-4.03×10^1	8.09

Table I: Solution of the linear system.

Currents Distribution

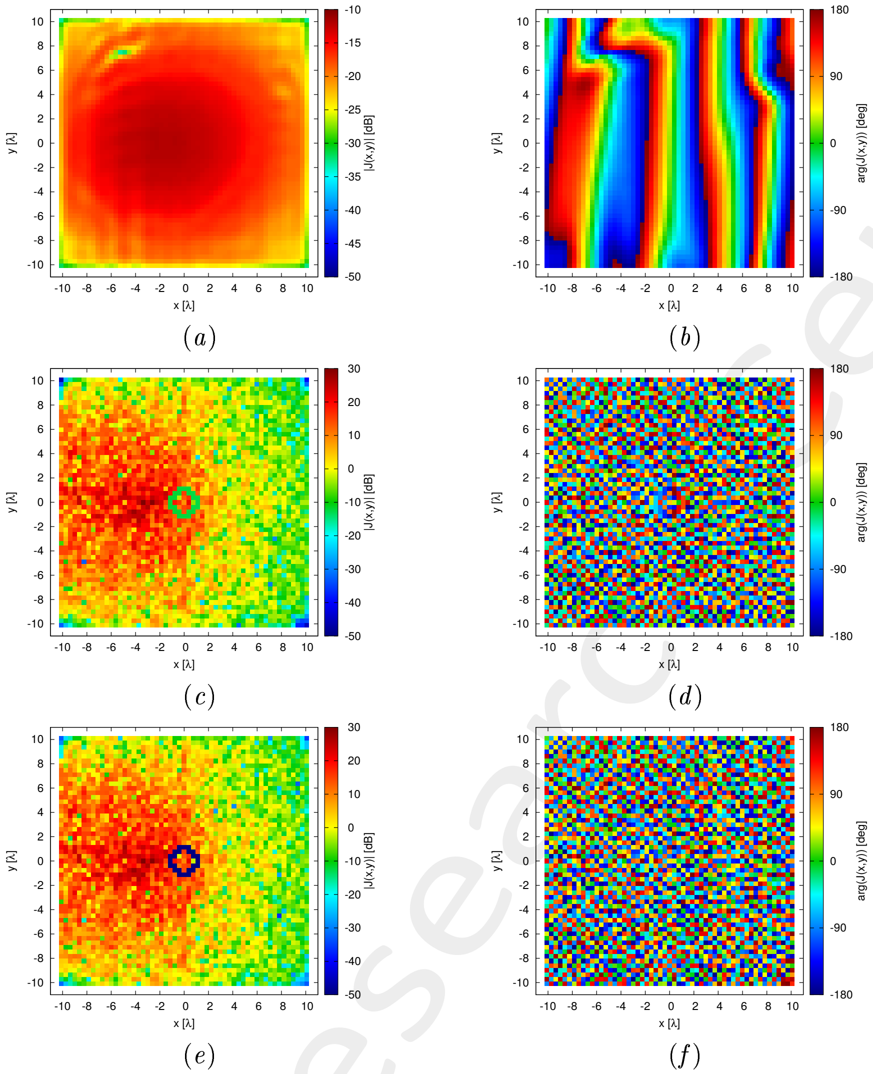

Figure 3: $(a)(c)(e)$ Magnitude and $(b)(d)(f)$ phase $(a)(b)$ of $J^{MN}(x,y)$, $(c)(d)$ $J^{NR}(x,y;\underline{\alpha})$, and $(e)(f)$ $J^{TOT}(x,y;\underline{\alpha})$.

Radiated Field

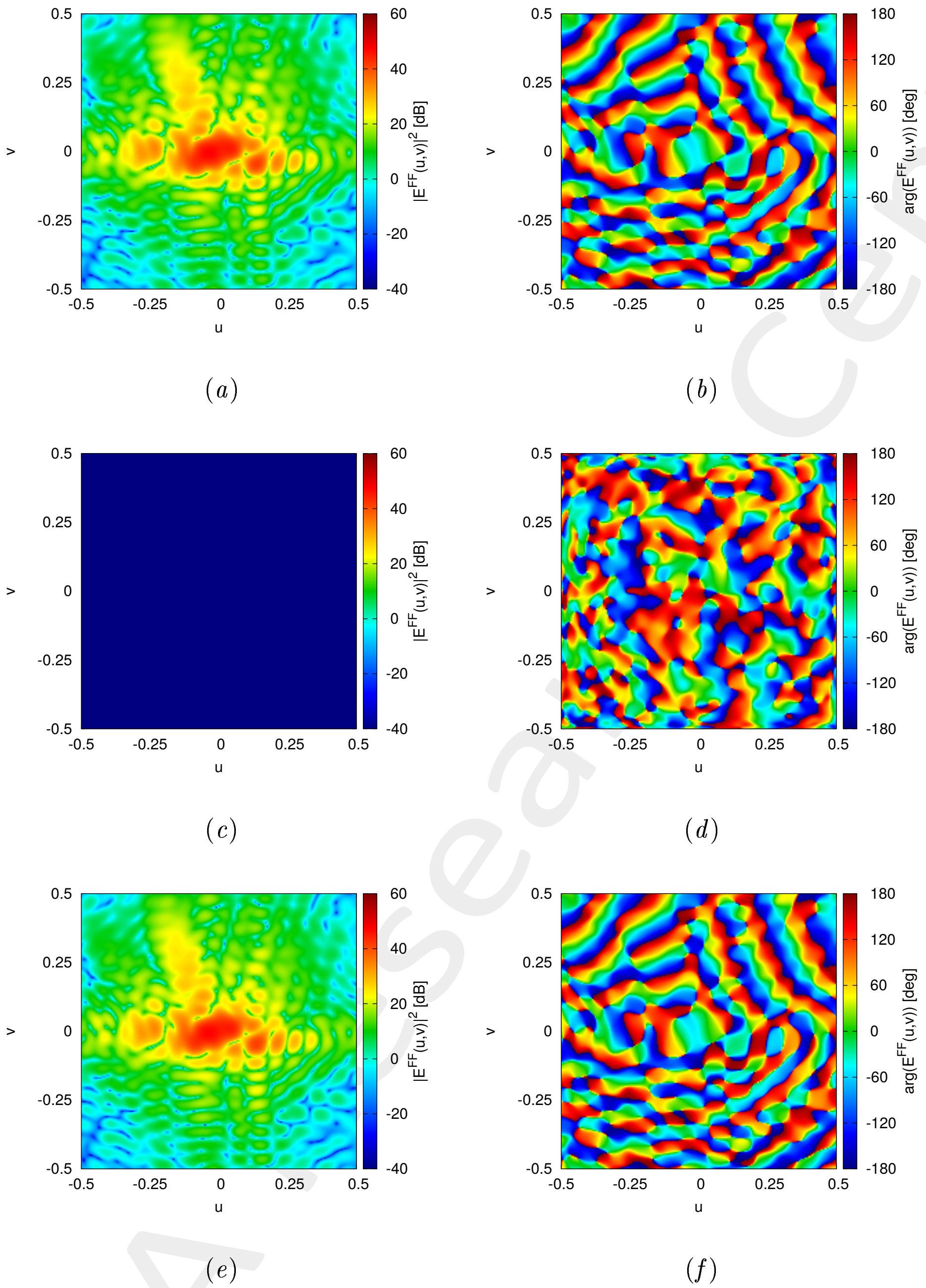

Figure 4: $(a)(c)(e)$ Magnitude and $(b)(d)(f)$ phase of the radiated field by $(a)(b)$, $J^{MN}(x,y)$, $(c)(d)$ $J^{NR}(x,y;\underline{\alpha})$, and $(e)(f)$ $J^{TOT}(x,y;\underline{\alpha})$.

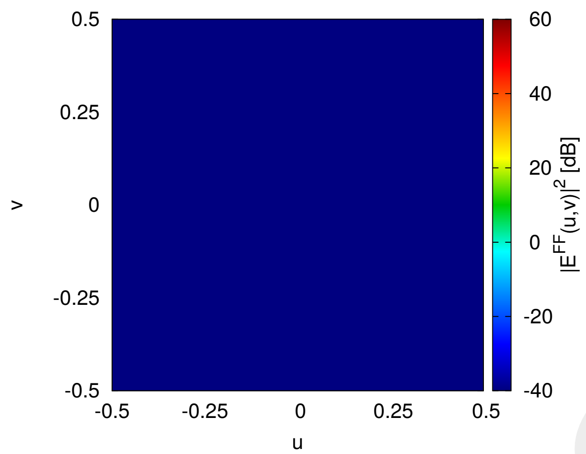

Figure 5: Magnitude of the difference between the radiated fields by $J^{MN}(x,y)$ and $J^{TOT}(x,y;\underline{\alpha})$.

1.2 Shape "2 O @ Center and up right corner"

Parameters

- Number of reflectarray elements: $M = N = 55$;
- Operative frequency: $f = 14$ [GHz];
- Polarization: X-CO;
- Number of elements in the forbidden region: $Q = 36$;

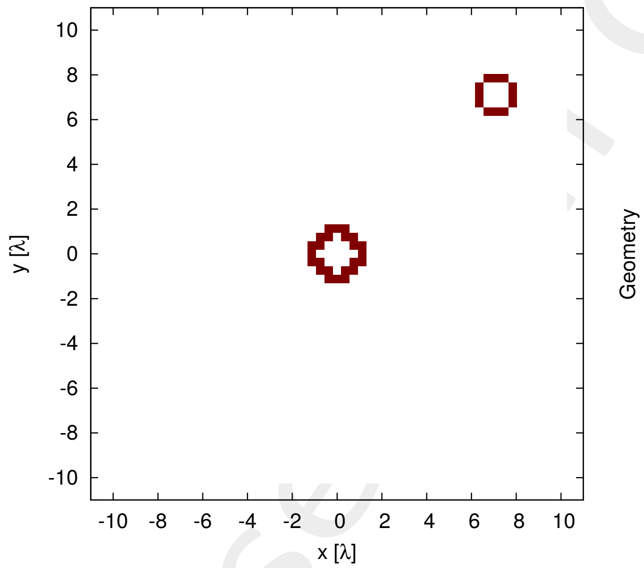

Figure 6: Geometry of forbidden region Ω.

Results

Magnitude and phase of the *NR* coefficients.

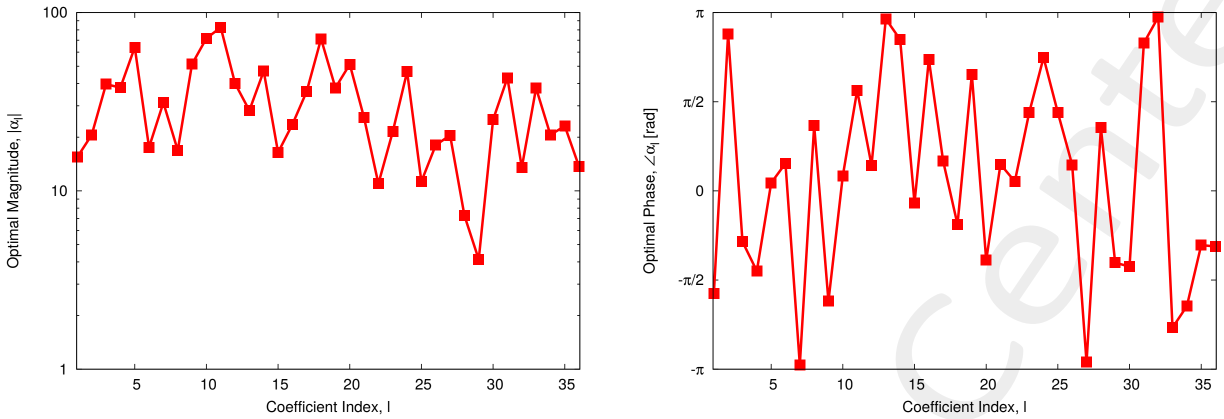

(a) (b)

Figure 7: Magnitude (a) and phase (b) of the solution.

Index q	$\Re\{\alpha_q\}$	$\Im\{\alpha_q\}$	Index q	$\Re\{\alpha_q\}$	$\Im\{\alpha_q\}$	Index q	$\Re\{\alpha_q\}$	$\Im\{\alpha_q\}$
1	-3.67	-1.51×10^1	13	-2.81×10^1	3.12	25	2.13	1.11×10^1
2	-1.92×10^1	7.51	14	-4.18×10^1	2.15×10^1	26	1.62×10^1	8.02
3	2.48×10^1	-3.09×10^1	15	1.61×10^1	-3.44	27	-2.03×10^1	-2.53
4	5.99	-3.75×10^1	16	-1.60×10^1	1.74×10^1	28	3.21	6.52
5	6.33×10^1	9.04	17	3.12×10^1	1.81×10^1	29	1.24	-3.93
6	1.55×10^1	8.17	18	5.92×10^1	-3.97×10^1	30	5.93	-2.44×10^1
7	-3.12×10^1	-2.45	19	-1.75×10^1	3.35×10^1	31	-3.71×10^1	2.19×10^1
8	6.86	1.54×10^1	20	1.75×10^1	-4.82×10^1	32	-1.35×10^1	1.08
9	-1.87×10^1	-4.79×10^1	21	2.30×10^1	1.16×10^1	33	-2.81×10^1	-2.52×10^1
10	6.91×10^1	1.88×10^1	22	1.08×10^1	1.82	34	-9.15	-1.85×10^1
11	-1.64×10^1	8.10×10^1	23	4.12	2.11×10^1	35	1.34×10^1	-1.89×10^1
12	3.60×10^1	1.75×10^1	24	-3.28×10^1	3.32×10^1	36	7.64	-1.14×10^1

Table II: Solution of the linear system.

Currents Distribution

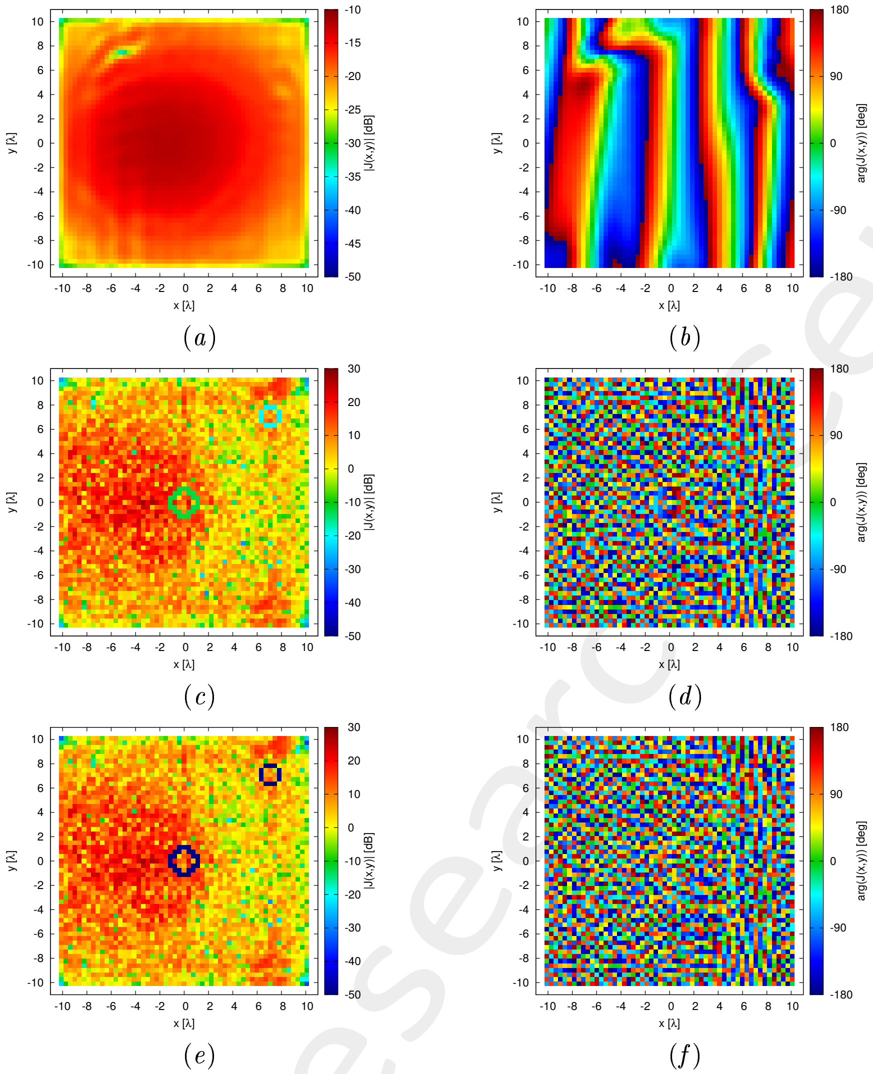

Figure 8: $(a)(c)(e)$ Magnitude and $(b)(d)(f)$ phase $(a)(b)$ of $J^{MN}(x,y)$, $(c)(d)$ $J^{NR}(x,y;\underline{\alpha})$, and $(e)(f)$ $J^{TOT}(x,y;\underline{\alpha})$.

Radiated Field

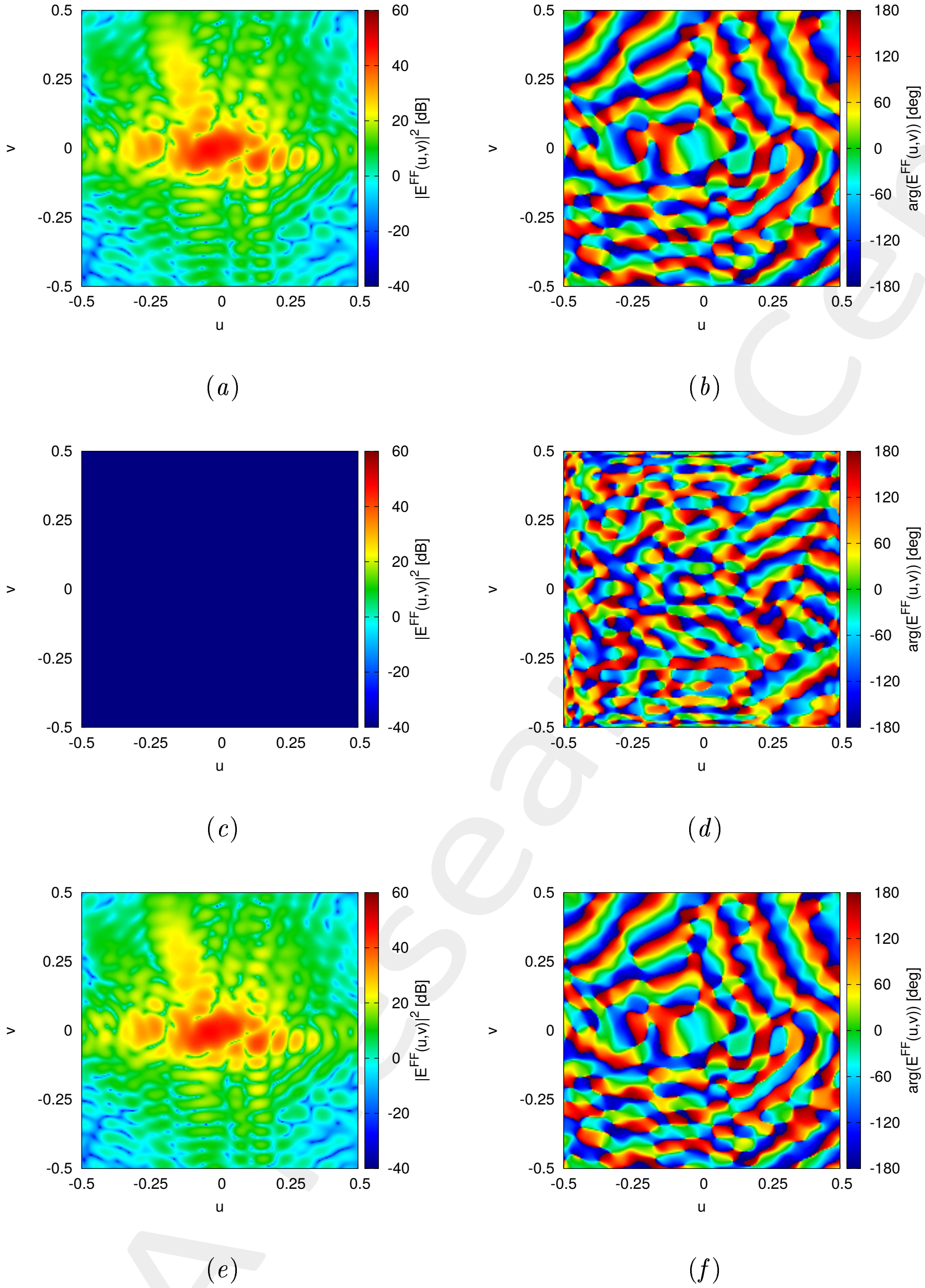

Figure 9: $(a)(c)(e)$ Magnitude and $(b)(d)(f)$ phase of the radiated field by $(a)(b)$, $J^{MN}(x,y)$, $(c)(d)$ $J^{NR}(x,y;\underline{\alpha})$, and $(e)(f)$ $J^{TOT}(x,y;\underline{\alpha})$.

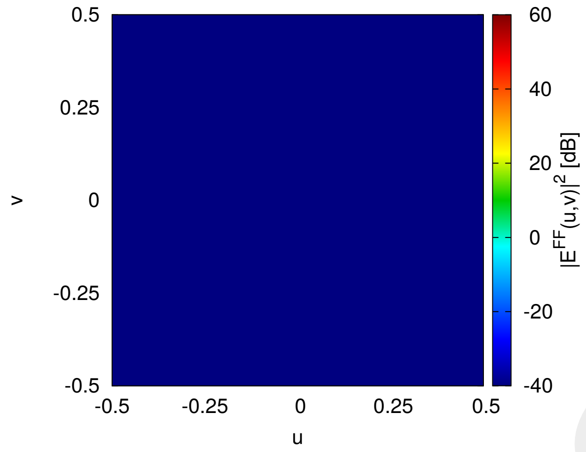

Figure 10: Magnitude of the difference between the radiated fields by $J^{MN}(x,y)$ and $J^{TOT}(x,y;\underline{\alpha})$.

1.3 Shape "2 Circle @ Center and up right corner"

Parameters

- Number of reflectarray elements: $M = N = 55$;
- Operative frequency: $f = 14$ [GHz];
- Polarization: X-CO;
- Number of elements in the forbidden region: $Q = 58$;
- $O = 58$.

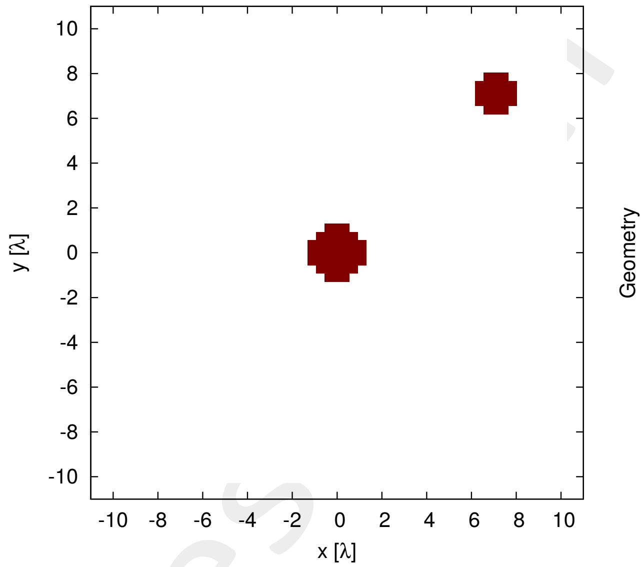

Figure 11: Geometry of forbidden region Ω.

Results

Magnitude and phase of the *NR* coefficients.

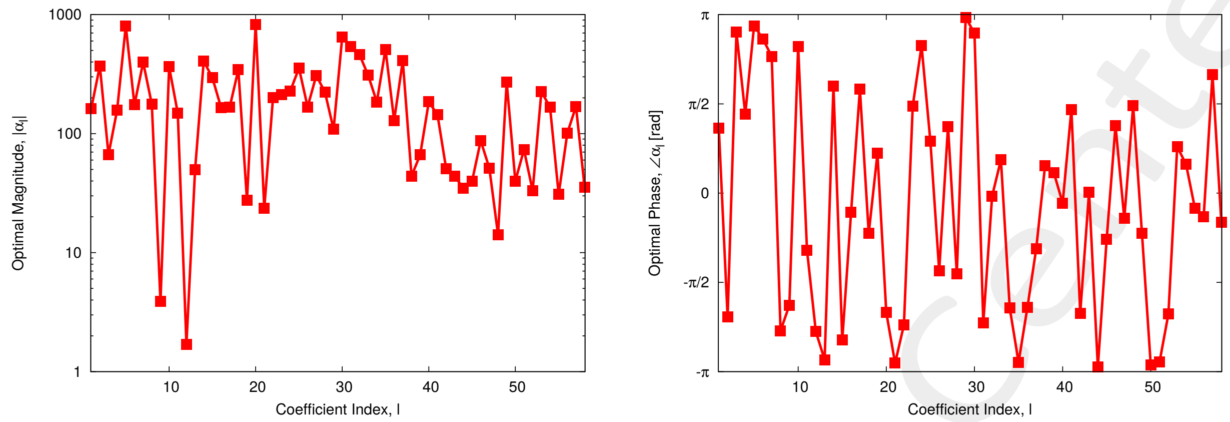

(a) (b)

Figure 12: Magnitude (a) and phase (b) of the solution.

Index q	$\Re\{\alpha_q\}$	$\Im\{\alpha_q\}$	Index q	$\Re\{\alpha_q\}$	$\Im\{\alpha_q\}$	Index q	$\Re\{\alpha_q\}$	$\Im\{\alpha_q\}$
1	6.66×10^1	1.47×10^2	21	-2.34×10^1	-3.53	40	1.82×10^2	-3.24×10^1
2	-2.12×10^2	-3.03×10^2	22	-1.37×10^2	-1.47×10^2	41	1.40×10^1	1.44×10^2
3	-6.34×10^1	2.03×10^1	23	7.56	2.12×10^2	42	-2.63×10^1	-4.36×10^1
4	2.81×10^1	1.55×10^2	24	-1.95×10^2	1.19×10^2	43	4.38×10^1	7.01×10^{-1}
5	-7.88×10^2	1.58×10^2	25	2.17×10^2	2.81×10^2	44	-3.46×10^1	-2.86
6	-1.59×10^2	7.21×10^1	26	3.40×10^1	-1.64×10^2	45	2.75×10^1	-2.90×10^1
7	-2.94×10^2	2.67×10^2	27	1.19×10^2	2.84×10^2	46	3.25×10^1	8.09×10^1
8	-1.33×10^2	-1.16×10^2	28	3.36×10^1	-2.21×10^2	47	4.61×10^1	-2.21×10^1
9	-1.52	-3.58	29	-1.08×10^2	5.89	48	4.67×10^{-1}	1.41×10^1
10	-3.09×10^2	1.93×10^2	30	-6.16×10^2	2.07×10^2	49	2.07×10^2	-1.75×10^2
11	8.00×10^1	-1.25×10^2	31	-3.52×10^2	-4.06×10^2	50	-3.97×10^1	-4.58
12	-1.29	-1.10	32	4.60×10^2	-2.49×10^1	51	-7.22×10^1	-1.27×10^1
13	-4.87×10^1	-1.03×10^1	33	2.57×10^2	1.72×10^2	52	-1.75×10^1	-2.81×10^1
14	-1.26×10^2	3.87×10^2	34	-8.06×10^1	-1.66×10^2	53	1.54×10^2	1.63×10^2
15	-2.50×10^2	-1.56×10^2	35	-5.04×10^2	-8.42×10^1	54	1.46×10^2	8.15×10^1
16	1.57×10^2	-5.44×10^1	36	-5.55×10^1	-1.17×10^2	55	2.99×10^1	-8.08
17	-4.24×10^1	1.61×10^2	37	2.28×10^2	-3.40×10^2	56	9.26×10^1	-4.08×10^1
18	2.62×10^2	-2.24×10^2	38	3.91×10^1	2.03×10^1	57	-8.35×10^1	1.47×10^2
19	2.11×10^1	1.77×10^1	39	6.21×10^1	2.34×10^1	58	3.08×10^1	-1.75×10^1
20	-4.16×10^2	-7.11×10^2						

Table III: Solution of the linear system.

Currents Distribution

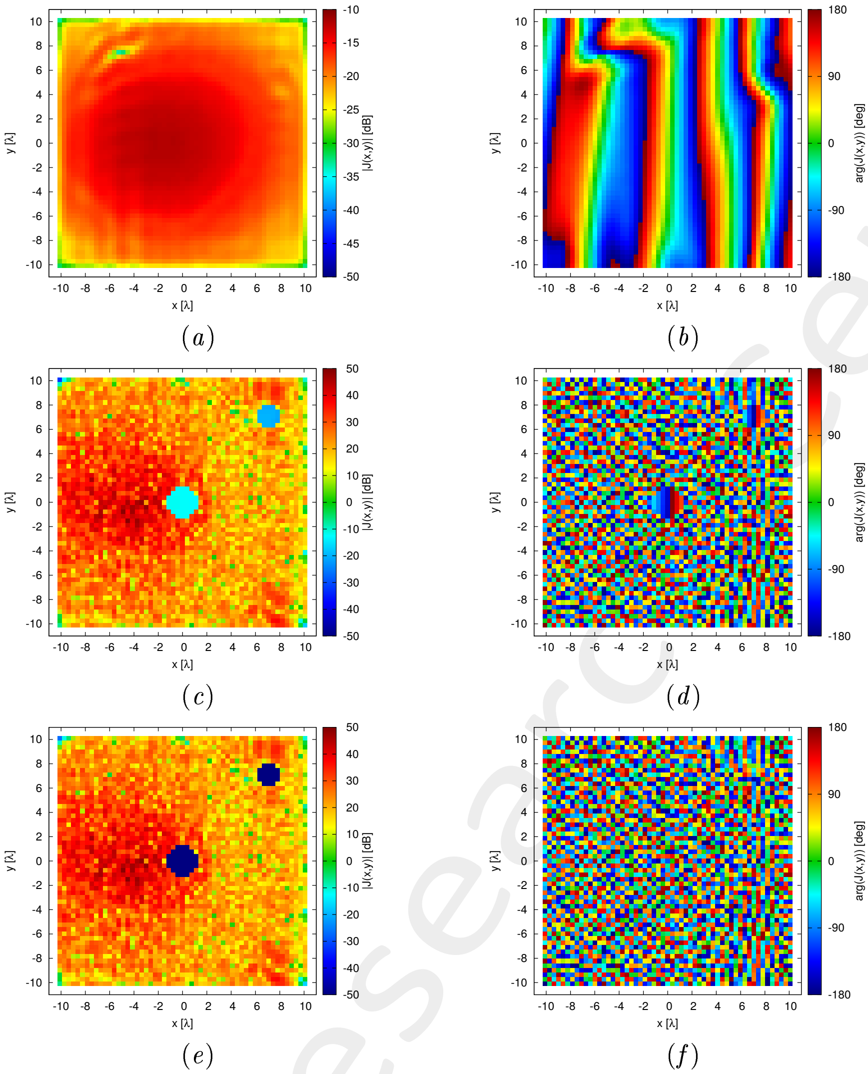

Figure 13: $(a)(c)(e)$ Magnitude and $(b)(d)(f)$ phase $(a)(b)$ of $J^{MN}(x,y)$, $(c)(d)$ $J^{NR}(x,y;\underline{\alpha})$, and $(e)(f)$ $J^{TOT}(x,y;\underline{\alpha})$.

Radiated Field

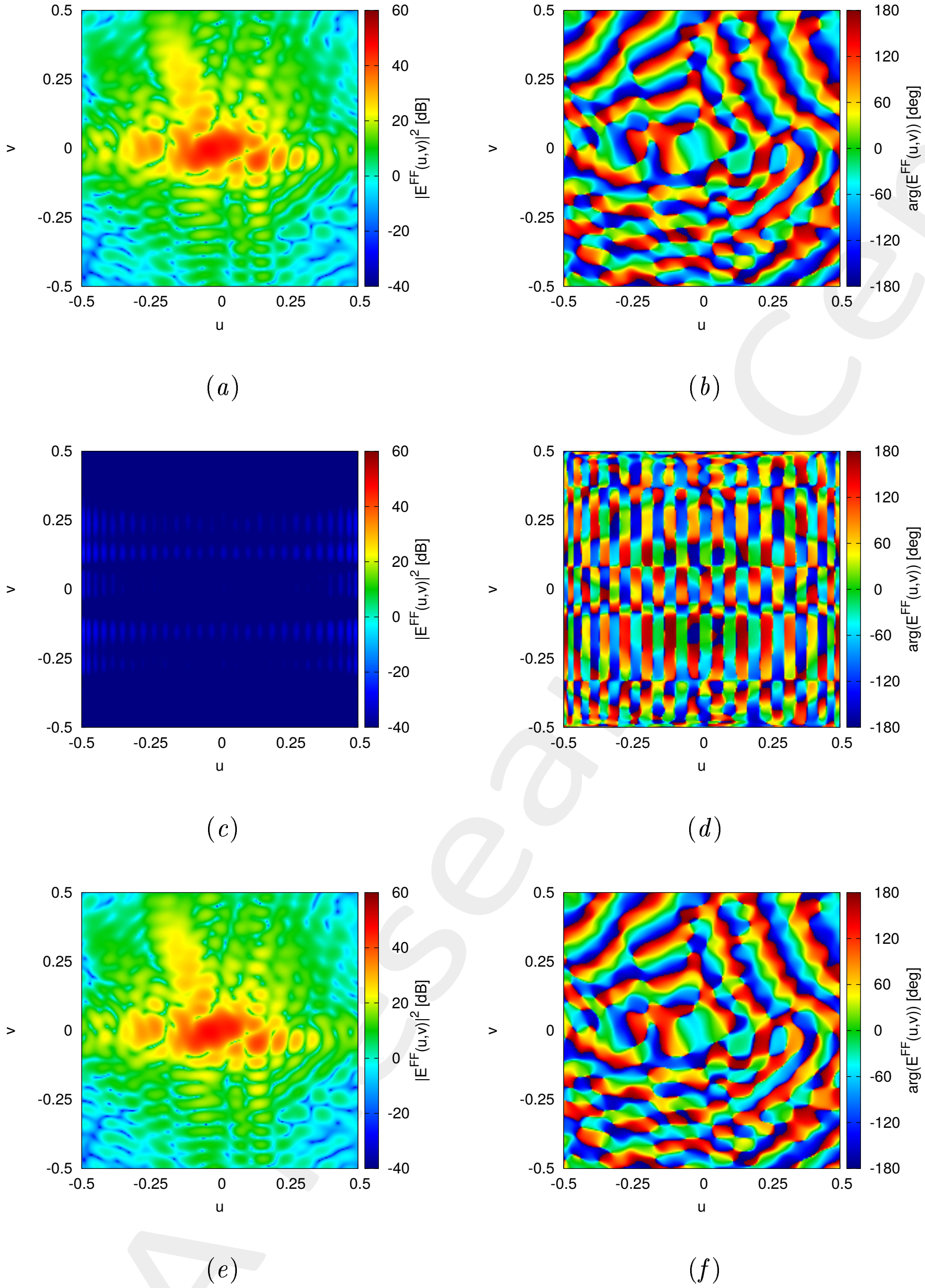

Figure 14: $(a)(c)(e)$ Magnitude and $(b)(d)(f)$ phase of the radiated field by $(a)(b)$, $J^{MN}(x,y)$, $(c)(d)$ $J^{NR}(x,y;\underline{\alpha})$, and $(e)(f)$ $J^{TOT}(x,y;\underline{\alpha})$.

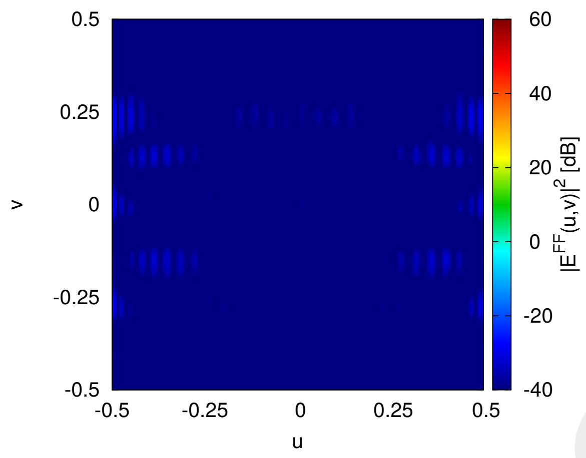

Figure 15: Magnitude of the difference between the radiated fields by $J^{MN}(x,y)$ and $J^{TOT}(x,y;\underline{\alpha})$.

References

[1] P. Rocca, G. Oliveri, R. J. Mailloux, and A. Massa, “Unconventional phased array architectures and design methodologies: A review,” *Proc. IEEE*, vol. 104, no. 3, pp. 544-560, Mar. 2016.

[2] P. Rocca, L. Poli, N. Anselmi, M. Salucci, and A. Massa, “Predicting antenna pattern degradations in microstrip reflectarrays through interval arithmetic,” *IET Microw., Antennas Propag.*, vol. 10, no. 8, pp. 817-826, Mar. 2016.

[3] M. Salucci, L. Tenuti, G. Oliveri, and A. Massa, “Efficient prediction of the EM response of reflectarray antenna elements by an advanced statistical learning method,” *IEEE Trans. Antennas Propag.*, vol. 66, no. 8, pp. 3995-4007, Aug. 2018.

[4] M. Salucci, A. Gelmini, G. Oliveri, N. Anselmi, and A. Massa, “Synthesis of shaped beam reflectarrays with constrained geometry by exploiting non-radiating surface currents,” *IEEE Trans. Antennas Propag.*, vol. 66, no. 11, pp. 5805-5817, Nov. 2018

[5] G. Oliveri, Y. Zhong, X. Chen, and A. Massa, “Multi-resolution subspace-based optimization method for inverse scattering,” *J. Opt. Soc. Amer. A*, Opt. Image Sci., vol. 28, no. 10, pp. 2057-2069, Oct. 2011.

[6] L. Poli, G. Oliveri, F. Viani, and A. Massa, “MT-BCS-based microwave imaging approach through minimum-norm current expansion,” *IEEE Trans. Antennas Propag.*, vol. 61, no. 9, pp. 4722-4732, Sep. 2013.

[7] N. Anselmi, P. Rocca, M. Salucci, and A. Massa, “Irregular phased array tiling by means of analytic schemata-driven optimization,” *IEEE Trans. Antennas Propag.*, vol. 65, no. 9, pp. 4495-4510, Sep. 2017.

[8] L. Poli, P. Rocca, M. Salucci, and A. Massa, “Reconfigurable thinning for the adaptive control of linear arrays,” *IEEE Trans. Antennas Propag.*, vol. 61, no. 10, pp. 5068-5077, Oct. 2013.

[9] L. Poli, G. Oliveri, P. Rocca, M. Salucci, and A. Massa, "Long-Distance WPT Unconventional Arrays Synthesis" *Journal of Electromagnetic Waves and Applications*, vol. 31, no. 14, pp. 1399-1420, Jul. 2017.

[10] M. Salucci, G. Gottardi, N. Anselmi, and G. Oliveri, “Planar thinned array design by hybrid analytical-stochastic optimization,” *IET Microwaves, Antennas & Propagation*, vol. 11, no. 13, pp. 1841-1845, Oct. 2017.

[11] P. Rocca, T. Moriyama, N. Anselmi, and A. Massa, “Robust prediction of the radiated pattern features with uncertainties in reflectarray design,” 2014 IEEE Antenna Conference on Antenna Measurements and Applications (IEEE CAMA 2014), Antibes Juan-les-Pins, France, pp. 1-3, November 16-19, 2014.

[12] G. Oliveri, A. Gelmini, M. Salucci, D. Bresciani, and A. Massa, “Exploiting non-radiating currents in reflectarray antenna design,” 11th European Conference on Antennas and Propagation (EUCAP 2017), Paris, France, pp. 88-91, March 19-24, 2017.